

Medium-Dependent Self-Assembly of an Amphiphilic Peptide: Direct Observation of Peptide Phase Domains at the Air–Water Interface

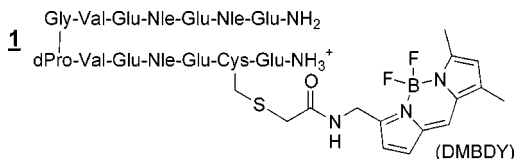
Evan T. Powers and Jeffery W. Kelly*

Department of Chemistry and the Skaggs Institute of
Chemical Biology, The Scripps Research Institute
10550 North Torrey Pines Road MB12
La Jolla, California 92037

Received August 16, 2000

A number of systems have been designed or discovered in which a peptide assembles when its environment is changed. The required change can result from active manipulation, as in pH-induced nanotube formation by cyclic peptides,¹ or salt-induced fibril formation by peptides or peptidomimetics.² It can also result from passive transfer of a peptide from one medium into another. For example, the fungal peptide alamethicin is monomeric in solution, but spontaneously self-assembles into pores in lipid bilayers.³ Herein we report a system of this latter type, where a soluble, monomeric peptide self-assembles upon partitioning to the air–water (A–W) interface. Peptide domains were directly detected, and some of their properties deduced, by fluorescence microscopy.

The peptide of interest, hereafter **1**, consists of two strands of alternating hydrophobic and hydrophilic residues centered on a putative D-Pro-Gly type II' β -turn⁴ (see below).



Peptide **1** should form an amphiphilic β -hairpin at the A–W interface, forcing the hydrophobic and hydrophilic side-chains to opposite sides of the molecule.⁵ The cysteine thiol was labeled with the 5,7-dimethyl derivative of the BODIPY (Molecular Probes) fluorophore (DMBDY) for concentration determination and to enable fluorescence microscopy studies.⁶

The CD spectrum of **1** (9 μ M) in deionized water⁷ (DIW) has a minimum at 198 nm,⁸ consistent with the peptide being unstructured.⁹ Equilibrium analytical ultracentrifugation (AUC) data for **1** (11 μ M) in DIW (Figure 1, left) fit a single ideal species model with an apparent molecular weight of 1750 g/mol (1875.9 g/mol expected for monomer). Similar results without the pattern evident in the residuals of Figure 1 (likely due to

(1) Ghadiri, M. R.; Granja, J. R.; Milligan, R. A.; McRee, D. E.; Khazanovich, N. *Nature* **1993**, *366*, 324–327.

(2) (a) Zhang, S.; Altman, M. *React. Funct. Polym.* **1999**, *41*, 91–102. (b) Lashuel, H. A.; Labrenz, S. R.; Woo, L.; Serpell, L. C.; Kelly, J. W. *J. Am. Chem. Soc.* **2000**, *122*, 5262–5277.

(3) (a) Schwarz, G.; Stankowski, S.; Rizzo, V. *Biochim. Biophys. Acta* **1986**, *861*, 141–151. (b) Rizzo, V.; Stankowski, S.; Schwarz, G. *Biochemistry* **1987**, *26*, 2751–2759.

(4) (a) Karle, I.; Awasthi, S. K.; Balam, P. *Proc. Natl. Acad. Sci. U.S.A.* **1996**, *93*, 8189–8193. (b) Stanger, H. E.; Gellman, S. H. *J. Am. Chem. Soc.* **1998**, *120*, 4236–4237.

(5) (a) DeGrado, W. F.; Lear, J. D. *J. Am. Chem. Soc.* **1985**, *107*, 7684–7689. (b) Boncheva, M.; Vogel, H. *Biophys. J.* **1997**, *73*, 1056–1072. (c) Maget-Dana, R.; Lelièvre, D.; Brack, A. *Biopolymers* **1999**, *49*, 415–423.

(6) $\epsilon = 58\,000\text{ M}^{-1}\text{ cm}^{-1}$ at $\lambda_{\text{max}} = 500\text{ nm}$, emission $\lambda_{\text{max}} = 510\text{ nm}$ in H₂O. See Supporting Information for the determination of ϵ .

(7) Initial studies of **1** were carried out in DIW so that its behavior could be studied in the absence of salt effects. The effects of pH and buffer on this system will be studied explicitly in future work.

(8) See Supporting Information

(9) Greenfield, N.; Fasman, G. D. *Biochemistry* **1969**, *8*, 4108–4116.

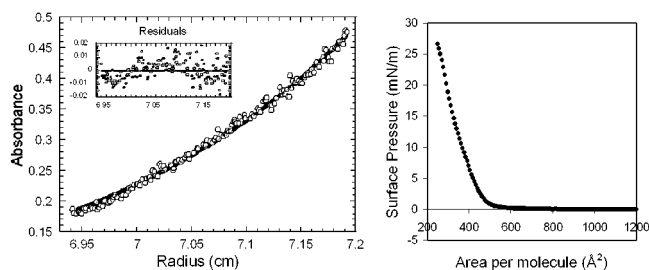


Figure 1. (Left) Equilibrium AUC data for **1** in DIW (11 μ M) at 50 000 rpm and 25 $^{\circ}$ C. (Right) Surface pressure vs area isotherm for **1** on DIW.⁸

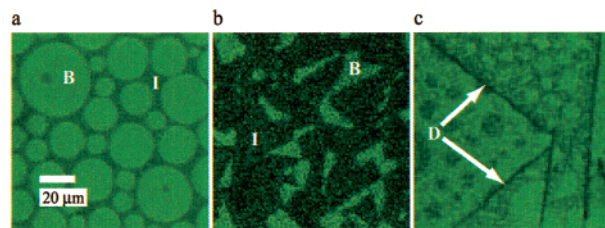


Figure 2. The surfaces of three different solutions of **1** viewed at 20 \times by confocal fluorescence microscopy, showing bright (B), intermediate (I), and dim (D) domains (excitation: 488 nm, detection: 522 nm). These are representative of 13 experiments with three separate preparations of **1**. All images are on the same scale.

nonideality at low ionic strength¹⁰) are obtained in 10 mM NaCl (MW = 1864 g/mol).⁸

The accumulation of amphiphilic peptides at the A–W interface is often demonstrated by injecting them into water and measuring the surface pressure of the solution's A–W interface.¹¹ When **1** (0.56 nmol) was injected into DIW (2 mL), the surface pressure rose from 0 to 10.5 (\pm 0.5) mN/m over 8 h.⁸ In pressure versus area isotherms of spread monolayers of **1** (Figure 1) this surface pressure is attained at a surface concentration of 46 pmol/cm² (360 \AA^2 /molecule, or about 70% surface saturation⁸). Since the area of the A–W interface was 4.2 cm², about 0.19 nmol of **1** transferred to the interface (35% of the total).

To study the peptide at the A–W interface, droplets (25 μ L) of **1** in DIW (0.26 μ M) were placed on coverslips and their surfaces (areas \approx 0.5 cm²) examined by confocal fluorescence microscopy. Self-assembly was apparent from the presence of discrete domains, as shown in Figure 2. These can be categorized by their fluorescence as bright, intermediate, or dim. The bright domains had about 1.5–2.5 times the intermediate domains' fluorescence, and 2.5–5 times the dim domains' fluorescence. The dim domains always had needlelike shapes (Figure 2c). The bright and intermediate domains were sometimes circular (Figure 2a and c), and sometimes irregularly shaped (Figure 2b). Domains moved during observation, probably due to a combination of Brownian motion¹² and interfacial turbulence (the Marangoni effect).^{13,14} Figure 3, which shows the first and last images from a 90-min observation of a droplet surface, illustrates more profound changes.¹⁴ The intermediate domains became circular during the experiment, while the dim domains melted. As the changes only occurred in the illuminated region, they were probably due to adventitious heating.

(10) McRorie, D. K.; Voelker, P. J. *Self-Associating Systems in the Analytical Ultracentrifuge*; Beckman Instruments: Fullerton, CA, 1993; pp 24–27.

(11) Maget-Dana, R. *Biochim. Biophys. Acta* **1999**, *1462*, 109–140.

(12) McConnell, H. M.; Rice, P. A.; Benvegnu, D. J. *J. Phys. Chem.* **1990**, *94*, 8965–8968.

(13) Sterling, C. V.; Scriven, L. E. *AIChE J.* **1959**, *5*, 514–523.

(14) See <http://www.scripps.edu/skaggs/kelly/> for movies.

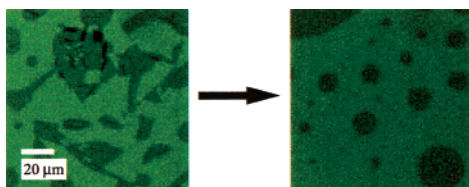


Figure 3. The $t = 0$ (left) and 90 min (right) images of the air–water interface of a solution of **1**. Over 90 min, the intermediate domains became circular, and the dim domains melted.¹⁴

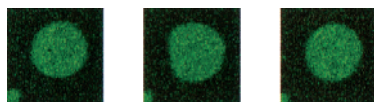


Figure 4. Successive images (at $20\times$) of a bright domain recorded 3 s apart.¹⁴ Domain shape fluctuation is apparent in the difference between the middle image and those on the right and left.

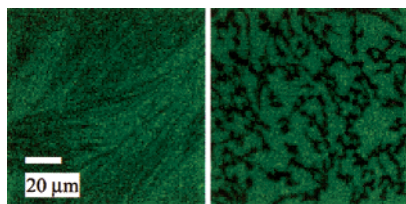


Figure 5. Fluorescence micrographs of $1.1\ \mu\text{M}$ solutions of **1** at $20\times$. The intermediate phase is not present, leaving only the bright phase and needles of the dim phase.

Showing that the self-assembly of **1** is conditional upon its transfer to the A–W interface requires demonstrations that it is monomeric in solution, that it transfers to the A–W interface, and that it self-assembles once there. The first task is accomplished by AUC (Figure 1), the second by time-dependent surface pressure measurements,⁸ and the third by the direct observation of domains (Figures 2 and 3). But what are the natures of the different domains? Why do they take the shapes seen in Figures 2 and 3? Some answers to these questions can be inferred from the domains' appearance and dynamics.

Three images of a bright domain recorded three seconds apart are shown in Figure 4. The domain's shape fluctuates, indicating that it is in a fluid state (intermediate domains behaved similarly).¹⁴ Furthermore, the bright and intermediate domains coexisted in the samples shown above, in which the maximum surface concentration was $16\ \text{pmol}/\text{cm}^2$ ($\sim 1000\ \text{\AA}^2/\text{molecule}$), and the corresponding surface pressure should be close to 0 mN/m. Under similar conditions, the two-dimensional (2D) equivalents of gas and liquid phases coexist in lipid monolayers.¹⁵ By analogy, and consistent with the fluidity noted above, the bright phase is likely the 2D liquid phase, and the intermediate phase, the 2D gas phase. This assumes that the denser liquid phase has the brighter fluorescence. However, collisional quenching or aggregation of the fluorophore¹⁶ could attenuate the fluorescence in the denser phase. The assignment was checked by examining droplets with a higher solution concentration ($1.1\ \mu\text{M}$) and therefore a higher surface concentration of **1**. Under such conditions, the liquid should become more prevalent at the expense of the gas. Indeed, the intermediate phase is absent as shown in Figure 5, leaving only the bright and dim phases. This supports the assignments made above; it also suggests that the dim domains

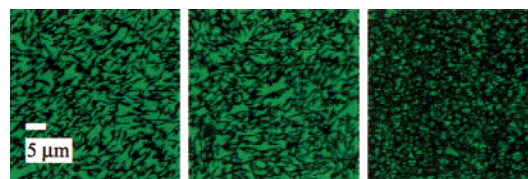


Figure 6. Fluorescence micrographs of Langmuir–Blodgett films of **1** on glass observed at $63\times$. The amount of the dim phase increases with the surface pressure at which the films were deposited, from 1 mN/m (left) to 10 mN/m (middle), to 20 mN/m (right).

are composed of a more condensed phase in which fluorescence is quenched. Several aspects of the dim domains indicate that they are in fact a 2D solid phase: they do not fluctuate, they melt when heated (Figure 3), and they are more abundant at higher surface pressures. Figure 6 illustrates this last point in showing spread monolayers deposited on hydrophilic glass substrates at 1, 10, and 20 mN/m (33, 46, and $57\ \text{pmol}/\text{cm}^2$).

Insight into the peptide domain shapes can be gained by drawing an analogy between peptides and lipids. In lipid monolayers, domain shapes and sizes depend on a balance between electrostatic repulsion and line tension (the analogue of surface tension).¹⁷ Electrostatic repulsion arises from the like charges (or dipole orientations) of the molecules in a domain. It favors either small, elongated domains, or domains that contain inclusions of another phase. Line tension arises from attractive interactions (van der Waals, hydrogen bonding, etc.) between molecules in a domain, and favors large, circular domains. The compromise between these forces is evident in Figure 2. For example, in Figure 2a, line tension results in circular domains, but the electrostatic repulsion causes gas-phase inclusions within the liquid domains. In Figure 2b, the liquid domains are elongated but homogeneous. Figure 2c is similar to Figure 2a, except for the needles of the solid phase. The extremely elongated shapes of the solid domains suggest that electrostatics dominates line tension in them.

Figures 2–6 provide information on the phases that **1** can form but do not address their molecular structures. A film at 25 mN/m (in which the liquid and solid phases coexist), was transferred to a CaF_2 substrate and examined by FT-IR.⁸ A band at $1629\ \text{cm}^{-1}$ indicates a β -sheet structure in the film.¹⁸ However, it is unclear whether it is the liquid, the solid, or both phases that are β -sheet-rich because the technique lacks spatial resolution. Further studies will address this issue in addition to the means by which **1** self-assembles.

In summary, **1** is monomeric in solution but transfers spontaneously to the A–W interface where it self-assembles into discrete domains. Three types of domains (gas, liquid, and solid) were observed, whose shapes were dictated by a balance between electrostatic repulsions and line tension.

Acknowledgment. We thank S. Deechongkit, M. Petrassi (AUC), H. Razavi (NMR), H. Bekele, D. Millar, and S. I. Yang (helpful discussions). This work was supported by the NIH (GM 51105), the Skaggs Institute of Chemical Biology and the Lita Annenberg Hazen Foundation. E.T.P. thanks the NIH for an NRSA.

Supporting Information Available: Details for the characterization of **1**, the determination of ϵ for DMBDY, the measurement of surface pressures of solutions of **1**, the measurement of pressure–area isotherms, the deposition of Langmuir–Blodgett films, IR spectroscopy, fluorescence microscopy, and AUC (PDF). This material is available free of charge via the Internet at <http://pubs.acs.org>.

JA005281

(15) Gaines, G. L. *Insoluble Monolayers at Liquid–Gas Interfaces*; John Wiley and Sons: New York, 1966; Chapter 4.

(16) Lakowicz, J. R. *Principles of Fluorescence Spectroscopy*, 2nd ed.; Kluwer Academic/Plenum: New York, 1999; Chapters 8–9.

(17) McConnell, H. M. *Annu. Rev. Phys. Chem.* **1991**, *42*, 171–195.

(18) Pelton, J. T.; McLean, L. R. *Anal. Biochem.* **2000**, *277*, 167–176.